International Journal of Engineering & Technology, 7 (3.19) (2018) 72-80

International Journal of Engineering & Technology

Website: www.sciencepubco.com/index.php/IJET

Research paper

Hidden Data Embedding Method Based on the Image Projections Onto the Eigenvectors of Subinterval Matrices

E.G. Zhilyakov[1], A.A. Chernomorets[2], E.V. Bolgova[3], I.I. Oleynik[4], D.A. Chernomorets[5]

Belgorod State National Research University, 85 Pobeda St, Belgorod, 308015, Russia
E-mail: zhilyakov@bsu.edu.ru
chernomorets@bsu.edu.ru
bolgova_e@bsu.edu.ru
oleinik_i@bsu.edu.ru
daria013ch@yandex.ru

Abstract

We consider the new method of hidden data embedding based on the transform of the container-image using the apparatus of subinterval matrices of the cosine transform. The developed method deals with the analysis of the container-image projections onto the eigenvectors of subinterval matrices. A decisive rule for the choice of informative and non-informative image projections subsets based on a given significance level is proposed. The computational experiments results of projections partitioning into informative and non-informative subsets show that it is possible to obtain a different numbers of informative and non-informative projections subsets using different significance levels. It allows to implement a hidden embedding of different data amounts. The embedding data are represented by a binary sequence. In our method we proposed to implement the data embedding on the basis of a relative change of given projections values. To test the workability of the developed method computational experiments were carried out. Their results showed that the developed method allows to perform data recovery without distortion, and causes a slight distortions of the image containing the embedded data. Also we carried out comparative computational experiments to compare the results of the developed method application with the results of E. Koch and J. Zhao method and spread spectrum method. Their results showed that the developed method causes less distortions of the container-image than other ones.

Keywords: *subinterval hidden data embedding, subinterval matrices, eigenvectors, spatial frequencies interval, image projection*

1. Introduction

Images and video data are one of the main forms of information exchange today. In many cases images are subject of copyright protection that assume the possibility of their use monitoring, for example, on the base of hidden embedding of control data into an image. The problem of hidden data embedding can be solved by allocating of image various components and changing them in accordance with the hidden data [1-9]. The hidden data embedding can also be performed based on the apparatus of subband matrices [10-14].

The hidden data embedding methods assume change of the image-container pixel values or the results of their various transforms. It is known that the hidden data embedding methods [1, 2] based on the various transforms results (such as the discrete Fourier transform etc.) have the most resistance to external destruction of embedded data.

In this paper, we propose a hidden data embedding method based on the image-container transforms that use the apparatus of subinterval matrices [15-17] of cosine transform. The developed method is based on the analysis and modification of individual subsets of the container-image projections onto the subinterval matrices eigenvectors [16]. The main statements of developed method are described below.

2. Background

Consider an image as a matrix of real values $\Phi=(f_{ik})$, $i=1,2,...,N_1$, $k=1,2,...,N_2$, where matrix elements correspond to the brightness of the image pixels.

The theoretical principles of the developed method are based on the following representation of the image f_{ik}, $i=1,2,...,N_1$, $k=1,2,...,N_2$:

$$f_{ik}=\frac{4}{\pi^2}\int_0^{\pi}\int_0^{\pi} F^{\Phi}(u,v)\cos(u(i-\frac{1}{2}))\cos(v(k-\frac{1}{2}))dudv, \quad (1)$$

$$i=1,2,\ldots,N_1, k=1,2,\ldots,N_2,$$

in the basis of following orthogonal functions:

Copyright © 2018 Authors. This is an open access article distributed under the Creative Commons Attribution License, which permits unrestricted use, distribution, and reproduction in any medium, provided the original work is properly cited.

$\{\cos(u(i-\frac{1}{2}))\}$, $\{\cos(v(k-\frac{1}{2}))\}$,

$$i=1,2,\ldots,N_1,\ k=1,2,\ldots,N_2, \quad (2)$$

where $F^{\Phi}(u,v)$ – frequency response (the result of the cosine Fourier transform),

$$F^{\Phi}(u,v)=\sum_{i=1}^{N_1}\sum_{k=1}^{N_2} f_{ik}\cos(u(i-\frac{1}{2}))\cos(v(k-\frac{1}{2})), \quad (3)$$

u, v – the normalized spatial frequencies (SF) that are defined in the following area:

$$(u,v)\in D_{\pi}, \quad (4)$$

$$D_{\pi}=\{(u,v)\,|\,0\le u,v<\pi\}. \quad (5)$$

Let's introduce the concept of the energy part $E_{r_1r_2}(\Phi)$ of the image Φ for its cosine transformation,

$$E_{r_1r_2}(\Phi)=\frac{4}{\pi^2}\iint_{(u,v)\in V_{r_1r_2}}\left|F^{\Phi}(u,v)\right|^2 dudv, \quad (6)$$

which corresponds to a given spatial frequency interval $V_{r_1r_2}$ of the following shape:

$$V_{r_1r_2}=\{(u,v)\,|\,u_{r_1,1}\le u<u_{r_1,2};\ v_{r_2,1}\le v<v_{r_2,2}\},$$

$$V_{r_1r_2}\subset D_{\pi}. \quad (7)$$

It's possible to show that the value $\|\Phi\|^2$ of the image Φ energy

$$\|\Phi\|^2=\sum_{i=1}^{N_1}\sum_{k=1}^{N_2} f_{ik}^2, \quad (8)$$

can be represented as

$$\|\Phi\|^2=\sum_{r_1=1}^{R_1}\sum_{r_2=1}^{R_2} E_{r_1r_2}(\Phi), \quad (9)$$

under assumption that

$$u_{r_1,1}=(r_1-1)\frac{\pi}{R_1},\quad u_{r_1,2}=r_1\frac{\pi}{R_1},$$

$$r_1=1,2,\ldots,R_1, \quad (10)$$

$$v_{r_2,1}=(r_2-1)\frac{\pi}{R_2},\quad v_{r_2,2}=r_2\frac{\pi}{R_2},$$

$$r_2=1,2,\ldots,R_2. \quad (11)$$

where R_1 and R_2 – the amount of intervals along each frequency axes in D_{π} (5).

If we transform (6) using (3) and (7), we can obtain that

$$E_{r_1r_2}(\Phi)=tr(G_{r_1}\Phi H_{r_2}\Phi^T), \quad (12)$$

where tr() – matrix trace operation; the elements of the matrices $G_{r_1}=(g_{in}^{r_1}),\ i,n=1,2,...,N_1$, and $H_{r_2}=(h_{in}^{r_2}),\ i,n=1,2,...,N_2$, (we called them as subinterval matrices of cosine transform corresponding to a frequency interval $V_{r_1r_2}$ of the shape (7)) have the following values [15]:

$$g_{in}^{r_1}=a_{in}^{r_1}+\tilde{g}_{in}^{r_1}. \quad (13)$$

$$a_{in}^{r_1}=\begin{cases}\dfrac{\sin(u_{r_1,2}(i-n))-\sin(u_{r_1,1}(i-n))}{\pi(i-n)}, & i\ne n,\\[2ex] \dfrac{u_{r_1,2}-u_{r_1,1}}{\pi}, & i=n,\end{cases} \quad (14)$$

$$\tilde{g}_{in}^{r_1}=\frac{\sin(u_{r_1,2}(i+n-1))-\sin(u_{r_1,1}(i+n-1))}{\pi(i+n-1)}. \quad (15)$$

$$h_{in}^{r_2}=a_{in}^{r_2}+\tilde{h}_{in}^{r_2}. \quad (16)$$

$$a_{in}^{r_2}=\begin{cases}\dfrac{\sin(v_{r_2,2}(i-n))-\sin(v_{r_2,1}(i-n))}{\pi(i-n)}, & i\ne n,\\[2ex] \dfrac{v_{r_2,2}-v_{r_2,1}}{\pi}, & i=n,\end{cases} \quad (17)$$

$$\tilde{h}_{in}^{r_2}=\frac{\sin(v_{r_2,2}(i+n-1))-\sin(v_{r_2,1}(i+n-1))}{\pi(i+n-1)}. \quad (18)$$

3. Method

Let suppose that certain container-image is defined as a matrix $\Phi=(f_{ik})$, $i=1,2,...,N_1$, $k=1,2,...,N_2$, and a spatial frequencies interval $V_{r_1r_2}$ (7) is given. Then we can calculate subinterval matrices G_{r_1} and H_{r_2} corresponding to interval $V_{r_1r_2}$ whose dimensions are $N_1\times N_1$ and $N_2\times N_2$ appropriately.

It is known [15], that subinterval matrices G_{r_1} and H_{r_2} are real, symmetric matrices. Hence these matrices can be represented as the following decompositions:

$$G_{r_1}=Q_{r_1}L_{r_1}Q_{r_1}^T,\quad H_{r_2}=U_{r_2}M_{r_2}U_{r_2}^T, \quad (19)$$

where the columns of the matrices Q_{r_1} and U_{r_2} are the eigenvectors of the matrices G_{r_1} and H_{r_2}, the eigenvalues of the matrices G_{r_1} and H_{r_2} are allocated on the main diagonal of the matrices L_{r_1} and M_{r_2},

$$Q_{r_1} = (\vec{q}_1^{\,r_1}, \vec{q}_2^{\,r_1}, ..., \vec{q}_{N_1}^{\,r_1}), \quad U_{r_2} = (\vec{u}_1^{\,r_2}, \vec{u}_2^{\,r_2}, ..., \vec{u}_{N_2}^{\,r_2}), \quad (20)$$

$$L_{r_1} = diag(\lambda_1^{r_1}, \lambda_2^{r_1}, ..., \lambda_{N_1}^{r_1}),$$
$$M_{r_2} = diag(\mu_1^{r_2}, \mu_2^{r_2}, ..., \mu_{N_2}^{r_2}).$$

Consider the matrix $\Gamma^{r_1 r_2} = (\gamma_{ik}^{r_1 r_2})$, $i = 1,2,...,N_1$, $k = 1,2,...,N_2$,

$$\Gamma^{r_1 r_2} = Q_{r_1}^T \Phi U_{r_2}, \quad (21)$$

which elements $\gamma_{ik}^{r_1 r_2}$, $i = 1,2,...,N_1$, $k = 1,2,...,N_2$,

$$\gamma_{ik}^{r_1 r_2} = (\vec{q}_i^{\,r_1})^T \Phi \vec{u}_k^{\,r_2}, \quad (22)$$

can be considered as image Φ projections [2, 18] onto orthogonal eigenvectors $\vec{q}_i^{\,r_1}$, $i = 1,2,...,N_1$, and $\vec{u}_k^{\,r_2}$, $k = 1,2,...,N_2$, of subinterval matrices G_{r_1} and H_{r_2} corresponding to the given interval $V_{r_1 r_2}$.

Let's split the matrix $\Gamma^{r_1 r_2}$ into $S_1 \times S_2$ submatrices (projections subsets) $\Psi_{s_1 s_2}$, $s_1 = 1,2,...,S_1$, $s_2 = 1,2,...,S_2$, having the same dimension $(N_1/S_1) \times (N_2/S_2)$ (where S_1, S_2 – some constants) as follows: a separate matrix (a projections subset) $\Psi_{s_1 s_2}$ contains the projections $\gamma_{ik}^{r_1 r_2}$, $i = 1,2,...,N_1$, $k = 1,2,...,N_2$, which satisfy the following condition (Figure 1):

$$\Psi_{s_1 s_2} = \{\gamma_{ik}^{r_1 r_2} \mid (s_1 - 1)N_1/S_1 + 1 \le i \le s_1 N_1/S_1,$$
$$(s_2 - 1)N_2/S_2 + 1 \le k \le s_2 N_2/S_2\} \quad (23)$$

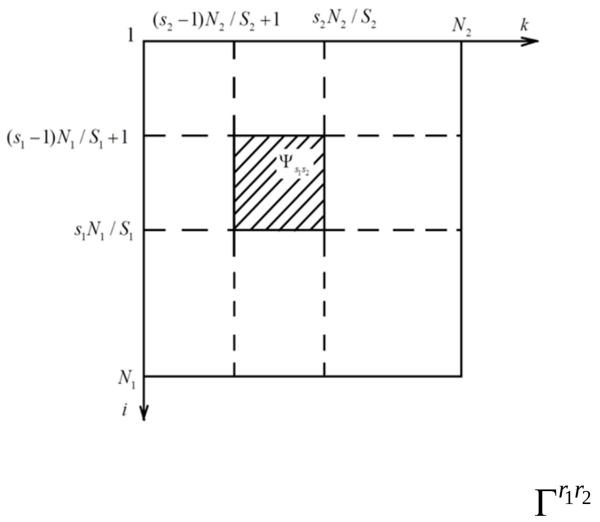

Figure 1: The projections subset $\Psi_{s_1 s_2}$

For each subset $\Psi_{s_1 s_2}$ we calculate the quantity $\Delta_{s_1 s_2}$ equal to the sum of the squared projections that belong to a given subset,

$$\Delta_{s_1 s_2} = \sum_{i=(s_1-1)N_1+1}^{s_1 N_1} \sum_{k=(s_2-1)N_2+1}^{s_2 N_2} \left|\gamma_{ik}^{r_1 r_2}\right|^2, \quad (24)$$

and the normalized value $\delta_{s_1 s_2}$,

$$\delta_{s_1 s_2} = \Delta_{s_1 s_2} / \sum_{i=1}^{N_1} \sum_{k=1}^{N_2} \left|\gamma_{ik}^{r_1 r_2}\right|^2. \quad (25)$$

Basing on the distribution of values $\delta_{s_1 s_2}$ (25) by subsets $\Psi_{s_1 s_2}$, $s_1 = 1,2,...,S_1$, $s_2 = 1,2,...,S_2$, we can formulate a decisive rule of finding for the informative and non-informative projections subsets as follows.

Consider the ordered set $W^{\Psi} = \{w_k^{\Psi}\}$, $k = 1,2,...,S_1 S_2$, where its elements are the values $\delta_{s_1 s_2}$ (25), $s_1 = 1,2,...,S_1$, $s_2 = 1,2,...,S_2$, in a decreasing order.

Let's set some quantity m^{Ψ} – the significance level of projections subsets,

$$0 < m^{\Psi} \le 1. \quad (26)$$

Let's calculate the value of the quantity $l_{m^{\Psi}}$,

$$1 \le l_{m^{\Psi}} \le S_1 S_2, \quad (27)$$

which corresponds to the following conditions:

$$\sum_{k=1}^{l_{m^{\Psi}}} w_k^{\Psi} \le m^{\Psi}, \quad \sum_{k=1}^{l_{m^{\Psi}}+1} w_k^{\Psi} > m^{\Psi}. \quad (28)$$

Let's create a set $Z_{m^{\Psi}} = \{(s_1, s_2)\}$ of subsets $\Psi_{s_1 s_2}$ indices corresponding to the first $l_{m^{\Psi}}$ elements of the ordered set W^{Ψ}.

Then, subsets $\Psi_{s_1 s_2}$, whose indices belong to the set $Z_{m^{\Psi}}$,

$$(s_1, s_2) \in Z_{m^{\Psi}}, \quad (29)$$

are called the informative projections subsets at the level m^{Ψ}.

Subsets $\Psi_{s_1 s_2}$, whose indices do not belong to the set $Z_{m^{\Psi}}$,

$$(s_1, s_2) \notin Z_{m^{\Psi}}, \quad (30)$$

are called non-informative projections subsets at the level m^{Ψ}.

Using (29), (30), we can construct a mask matrix $\Psi_{s_1 s_2}^{Mask, m^{\Psi}}$ of the corresponding informative and non-informative image projections subsets (we'll use it for the development of hidden data embedding method):

$$\Psi_{s_1 s_2}^{Mask,m^{\Psi}} = \begin{cases} 1, (s_1, s_2) \in Z_{m^{\Psi}}; \\ 0, (s_1, s_2) \notin Z_{m^{\Psi}}. \end{cases} \quad (31)$$

Examples of constructing a mask-matrix (31) of informative and non-informative projections subsets for a known image "Lena" for the various values m^{Ψ} ={0.9999, 0.9995, 0.998, 0.995} are shown in Figure 2 (here the projections set $\Gamma^{r_1 r_2}$ is dividing onto 8×8 subsets ($S_1 = S_2 = 8$)).

1	1	1	1	1	1
1	1	1	1	1	1
1	1	1	1	1	1
1	1	1	1	1	1
1	1	1	1	1	1
1	1	1	1	1	1
1	1	1	1	1	1
1	1	1	1	1	1

a

1	1	1	1	1	1
1	1	1	1	1	1
1	1	1	1	1	1
1	1	1	1	1	1
1	1	1	1	1	1
1	1	1	1	1	1
1	1	0	0	1	1
1	1	0	0	1	1

b

1	1	1	1	1	1
1	1	1	1	1	1
1	0	0	0	0	0
1	1	0	0	0	0
1	1	0	0	1	0
1	1	0	0	0	0
1	0	0	0	0	0
1	0	0	0	0	0

c

1	1	1	1	1	1	1	1
1	0	0	0	0	0	0	0
0	0	0	0	0	0	0	0
0	0	0	0	0	0	0	0
0	0	0	0	0	0	0	0
0	0	0	0	0	0	0	0
0	0	0	0	0	0	0	0
0	0	0	0	0	0	0	0

d

Figure 2: Mask of projections subsetssplitting into informative and non-informative subsets, $S_1 = S_2 = 8$:a) m^{Ψ} =0.9999, b) m^{Ψ} =0.9995, c) m^{Ψ} =0.998, d) m^{Ψ} =0.995

In Figure 2, the digit"1" indicates the informative projections subsets corresponding to given m^{Ψ} , and the digit "0" – non-informative projections subsets(they are recommended for data embedding).
The results (Figure 2) of computational experiments of projections subsets spliting into informative and non-informative subsets show that different values m^{Ψ} allow to obtain a different amount of informative and. This property allows to execute the hidden embedding of the different data amount using non-informative projections subsets.
In the developed method it is proposed to implement the hidden data embedding into non-informative subsets of image projections onto subinterval matrices eigenvectors basing on a relative changes of given pair projections values (22). The embedding data are represented by a zeros and ones sequence.

To execute hidden data embedding it is proposed to make relative changes of the two selected projections $\gamma_{ik}^{r_1 r_2}$ and $\gamma_{i,k+1}^{r_1 r_2}$ (22) of container-image Φ onto the eigenvectors of the subinterval matrices corresponding to a given interval $V_{r_1 r_2}$. Selected projections should also belong to the corresponding non-informative projections subsets (30). So after changing of selected projections, the following inequalities should be correct:

- if embedding "0" the following inequality must be fulfilled:

$$\left| \tilde{\gamma}_{ik}^{r_1 r_2} \right| \geq \left| \tilde{\gamma}_{i,k+1}^{r_1 r_2} \right| + T_{\gamma}^{s_1 s_2}, \quad (14)$$

- if embedding "1" the following inequality must be fulfilled:

$$\left| \tilde{\gamma}_{ik}^{r_1 r_2} \right| \leq \left| \tilde{\gamma}_{i,k+1}^{r_1 r_2} \right| - T_{\gamma}^{s_1 s_2}, \quad (15)$$

where $\tilde{\gamma}_{ik}^{r_1 r_2}$ and $\tilde{\gamma}_{i,k+1}^{r_1 r_2}$ are the modified values of the corresponding projections, $T_{\gamma}^{s_1 s_2}$ – the threshold of the relative difference between the changed projections.

It is obvious that the threshold $T_{\gamma}^{s_1 s_2}$ influences on the distortion of the container-image: the threshold increasing causes the image-container distortions increasing (the data hiding is reduced). It should also be noted that the threshold $T_{\gamma}^{s_1 s_2}$ influences on the stability of embedded data recovery (extraction): when the external destructive influence exists, for example, additive noise, threshold decreasing leads to the increasingof the extracted data distortions.

In this paper, in order to ensure the embedded data stability against the external destructive influences, as well as to ensure the secrecy of data embedded into the container-image, it is proposed to determine the threshold values $T_{\gamma}^{s_1 s_2}$ adaptively.

It is proposed to determine threshold $T_{\gamma}^{s_1 s_2}$ using the mean value of the projections belonging to the selected subset $\Psi_{s_1 s_2}$ in case of the data embedding into a projections subset $\Psi_{s_1 s_2}$. So threshold $T_{\gamma}^{s_1 s_2}$ should be defined as:

$$T_{\gamma}^{s_1 s_2} = t_{\gamma} \gamma_{cp}^{s_1 s_2}, \quad (34)$$

where t_{γ} – an embedding factor which allows to interactively revise the threshold $T_{\gamma}^{s_1 s_2}$; $\gamma_{cp}^{s_1 s_2}$ – the mean value of the projections belonging to the selected subset $\Psi_{s_1 s_2}$,

$$\gamma_{cp}^{s_1 s_2} = \sqrt{\frac{\Delta_{s_1 s_2}}{\frac{N_1}{S_1} \frac{N_2}{S_2}}}, \quad (35)$$

where $\Delta_{s_1 s_2}$ – the sum of the squared projections (24) belonging to the subset $\Psi_{s_1 s_2}$, $N_1 \times N_2$ –dimensions of the container-image Φ, $N_1 / S_1 \times N_2 / S_2$ – dimensions of the projections subset $\Psi_{s_1 s_2}$.

As an examplethe mean values (35) of the projections belonging to the subset $\Psi_{s_1 s_2}$, $s_1 = 1,2,...,S_1$, $s_2 = 1,2,...,S_2$, are given in Table 1. Projections are calculated for the known image "Lena" into given frequency intervals V_{11} and V_{13} , when $R_1 = R_2 = 4$, $N_1 = N_2 = 128$ and $S_1 = S_2 = 4$.

Table 1: Mean values of image "Lena" projection into given frequency intervals V_{11} and V_{13}

V_{11}					V_{13}			
s_1 \ s_2	1	2	3	4	1	2	3	4

1	423,513	39,454	18,243	19,634	19,509	121,356	118,995	390,347
2	28,349	7,938	6,979	6,774	5,959	10,680	13,516	25,080
3	11,977	6,783	7,659	6,512	6,382	7,102	10,440	9,506
4	11,398	6,529	7,432	6,565	5,740	6,681	10,248	9,396

The data given in Table 1 show that in different projections subsets the mean values of the projections $\gamma_{cp}^{s_1 s_2}$ (35) differ significantly. Hence, the corresponding threshold values $T_\gamma^{s_1 s_2}$ (34) will also differ significantly when embedding into the various projections subsets.This indicates the expediency of adaptive threshold determination. Adaptive threshold $T_\gamma^{s_1 s_2}$ determination allows to execute the data embedding that causes minor distortions of the container-image.

The proposed embedding/extraction method is as follows.

Let the embedding data are given in a binary form. It is necessary to perform hidden data embedding into a given of spatial frequencies interval $V_{r_1 r_2}$ (7) of container-image Φ using a given level

$$m^{\Psi} \quad (26).$$

Using the decision rule (29)-(30) we can determine the informative and non-informative projections subsets of the image-container Φ corresponding to level m^{Ψ}. Let the indices (s_1, s_2) of non-informative projections subsets form a set Z_s. In the set Z_s, the non-informative projections subsets are sorted in descending order of corresponding quantity (25). We propose to implement data embedding into non-informative projections subsets.

Consider the embedding process of binary data $B=(b_m)$, $m=1,2,...,N_B$, into a non-informative projections subset $\Psi_{s_1 s_2}$ of interval $V_{r_1 r_2}$.

Denote $Q_{s_1} = \{\vec{q}_i^{\,r_1}\}$ and $U_{s_2} = \{\vec{u}_k^{\,r_2}\}$ – sets of eigenvectors of subinterval matrices G_{r_1} and H_{r_2} corresponding to the projections of the subset $\Psi_{s_1 s_2}$,

$$(s_1-1)N_1/S_1+1 \le i \le s_1 N_1/S_1, \quad (36)$$

$$(s_2-1)N_2/S_2+1 \le k \le s_2 N_2/S_2. \quad (37)$$

Each bit of the sequence $B=(b_m)$, $m=1,2,...,N_B$, is embedded based on the relative change in of two projections with indexes (i,k) and $(i,k+1)$ satisfying the inequalities (36) and(37).

Consider the embedding of a separate bit b_m using eigenvectors pairs $\vec{q}_i^{\,r_1}$, $\vec{u}_k^{\,r_2}$ and $\vec{q}_i^{\,r_1}$, $\vec{u}_{k+1}^{\,r_2}$,

$$\vec{q}_i^{\,r_1} \in Q_{s_1},$$

$$\vec{u}_k^{\,r_2},\ \vec{u}_{k+1}^{\,r_2} \in U_{s_2}.$$

Projections (22) $\gamma_{ik}^{r_1 r_2}$ and $\gamma_{i,k+1}^{r_1 r_2}$ of container-image Φ onto selected eigenvectors pairs $\vec{q}_i^{\,r_1}$, $\vec{u}_k^{\,r_2}$ and $\vec{q}_i^{\,r_1}$, $\vec{u}_{k+1}^{\,r_2}$ are determined as:

$$\gamma_{ik}^{r_1 r_2} = \left(\vec{q}_i^{\,r_1}\right)^T \Phi \vec{u}_k^{\,r_2}, \quad (38)$$

$$\gamma_{i,k+1}^{r_1 r_2} = \left(\vec{q}_i^{\,r_1}\right)^T \Phi \vec{u}_{k+1}^{\,r_2}. \quad (39)$$

If the embedding bit b_m is 0, then the projections $\gamma_{ik}^{r_1 r_2}$ and $\gamma_{i,k+1}^{r_1 r_2}$ should be changed so that their changed values $\tilde{\gamma}_{ik}^{r_1 r_2}$ and $\tilde{\gamma}_{i,k+1}^{r_1 r_2}$ satisfy the inequality (32).

If the embedding bit b_m is 1, then the projections $\gamma_{ik}^{r_1 r_2}$ and $\gamma_{i,k+1}^{r_1 r_2}$ should be changed so that their changed values $\tilde{\gamma}_{ik}^{r_1 r_2}$ and $\tilde{\gamma}_{i,k+1}^{r_1 r_2}$ satisfy the inequality (33).

The data embedding into the container image Φ can be formulated in a matrix form when all possible bits are embedded into a projections subset $\Psi_{s_1 s_2}$:

$$\tilde{\Phi} = \Phi - Q_{s_1} Q_{s_1}^T \Phi U_{s_2} U_{s_2}^T + Q_{s_1} \tilde{\Psi}_{s_1 s_2} U_{s_2}^T. \quad (40)$$

where $\tilde{\Psi}_{s_1 s_2}$ – matrix of modified using (32) and (33) projections of subset $\Psi_{s_1 s_2}$; $\tilde{\Phi}$ – container-image containing embedded data.

To extract from the container-image $\tilde{\Phi}$ the value of a single embedded bit using the pairs of eigenvectors $\vec{q}_i^{\,r_1}$, $\vec{u}_k^{\,r_2}$ and $\vec{q}_i^{\,r_1}$, $\vec{u}_{k+1}^{\,r_2}$ we should check the rightness of corresponding inequality (32) or (33).

For the simultaneous data embedding using other pairs of eigenvectors or when embedding into other non-informative intervals the same actions as above are performed.

The hidden data embedding method into several projections subsets simultaneously can be formulated as follows:

$$\tilde{\Phi} = \Phi - \sum_{(s_1,s_2)\in Z_s} Q_{s_1} Q_{s_1}^T \Phi U_{s_2} U_{s_2}^T + \sum_{(s_1,s_2)\in Z_s} Q_{s_1} \tilde{\Psi}_{s_1 s_2} U_{s_2}^T . \quad (41)$$

While embedding into non-informative projections subsets $\Psi_{s_1 s_2}$, $(s_1, s_2) \in Z_s$, there is an exact data recovery, since the set of matrices $\{Q_{s_1}\}$, as well as the set of matrices $\{U_{s_2}\}$, $(s_1, s_2) \in Z_s$, used in (41), are formed by mutually orthogonal eigenvectors of subinterval matrices G_{r_1} and H_{r_2} appropriately.

4. Computational Experiments

4.1 The Developed Method Workability Testing

Computational experiments were carried out to verify the workability ofthe developed method.

The known image “Lena” was selected as the container-image. We set $N_1 = N_2 = 512$ and $R_1 = R_2 = 4$. An image of a dimension of 32×16 pixels was chosen for constructing of the embedding data (Figure 3a). A binary representation of the embedding data is shown in Figure 3b. The embedding data set contains 4096 bits. Level m^{Ψ} was chosen equal to m^{Ψ} =0.99. Interval V_{11} was chosen for embedding process. Coefficient t_{γ} (34) was chosen equal to t_{γ} =0.1. A non-informative projections subset of indices (3, 1) was used for embedding.

Figure 3c shows the result of the hidden data embedding into the container-image “Lena” (image-container distortions are undistinguished).

After extraction the recovered data have no distortion.

a b c

Figure 3: Results of embedding into the container-image “Lena”

a) the image used for embedding datasetforming b) binary representation of the embedding data; c) the image containing the embedded data (distortions are undistinguished)

The corresponding distortion of the container image has the following values:

- mean square error [18] is equal to 0.0184;

- structural similarity index [19] is equal to 0.9966.

The obtained results demonstrate the high efficiency of the developed hidden data embedding method.

4.2 Comparative Computational Experimentsplanning

Comparative computational experiments were conducted to estimate the data embedding hiding using the developed method. Known methods of steganography – the method of relative replacement of the DCT coefficients (Koch-Zhao method) [1] and the spread spectrum method [9] were used for comparison.

To compare the data embedding hiding the distortions of container-images containing the embedded data as compared to the original container-images were estimated using the following distortion measures:

- mean square error MSE:

$$MSE(\Phi, \tilde{\Phi}) = \sum_{i=1}^{N_1} \sum_{j=1}^{N_2} \left(f_{ij} - \tilde{f}_{ij}\right)^2 / \sum_{i=1}^{N_1} \sum_{j=1}^{N_2} f_{ij}^2, \quad (42)$$

where f_{ij}, $\tilde{f}_{ij}$, $i = 1,2,\ldots,N_1$, $j = 1,2,\ldots,N_2$, – brightness values of the pixels of the container-image Φ and $\tilde{\Phi}$ before and after the data embedding;

- structural similarity index SSIM, it was proposed in [19].

For the computational experiments images K1, K2 and K3 of a dimension 512×512 pixels were selected as the container-images (Fig. 4). These images were chosen because they have the different distribution of their energy parts (12) over the frequency intervals of the shape (7).

K1 K2 K3

Figure 4: Examples of container-images K1, K2 and K3

The binary representation of embedding data was constructed using the brightness values of the image B1 pixels (the dimension 32×16 pixels) (Fig. 5).

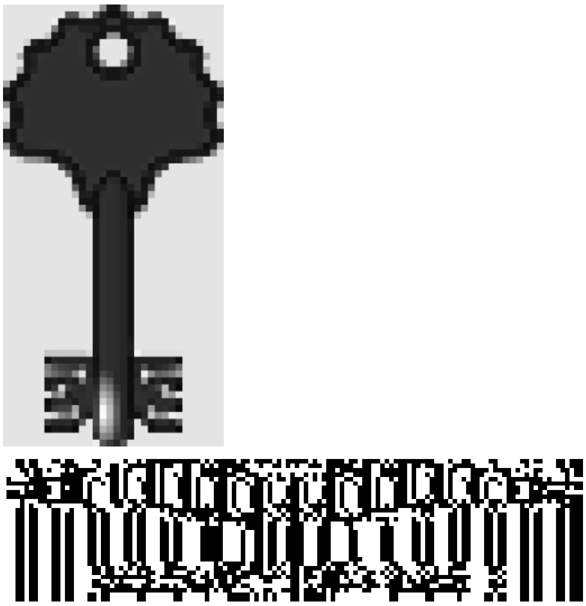

a

b

Figure 5: Embedding image B1

a) the image used for the embedding data forming;

b) binary representation of the embedding data

The embedding data amount is limited to 4096 bits as the Koch-Zhao method that was described in [1] does not allow the embedding the larger data amount into the container imagesof the given sizes. The frequency area is splitted into 8×8 spatial frequency intervals ($R_1 = R_2 = 8$). The partitioning by 8×8 subsets

($S_1 = S_2 = 8$) of the corresponding container-image projections set is carried out. Based on the preliminary calculations results the projections subsets $\Psi_{s_1 s_2}$, $s_1 = 1,2,\ldots,S_1$, $s_2 = 1,2,\ldots,S_2$, corresponding to the interval V_{11} of shape (7) is chosen.

To determine the non-informative projections subsets the value of projections subsets significance level (26) is chosen equal to m^{Ψ}=0.999.

The following values of the embedding coefficient t_γ are used (they allow to obtain the best embedding results):

-for image K1 – t_γ ={0.1; 0.2; 0.3};

-for image K2 – t_γ ={0.1; 0.15; 0.2};

-for image K3 – t_γ ={0.05; 0.1; 0.15}.

In the Koch-Zhao method, the recommended [1] threshold values P are used:

$$P = \{0.5;\quad 5;\quad 25\}.$$

In the spread spectrum method [9], the basic functions are constructed using corresponding blocks of pixels containing $B_s \times B_s$ elements (B_s is equal to 4 and 8). When using larger blocks, for example, 16×16 elements, the spread spectrum method does not allow to embed all given data into the selected container-images.

4.3 Comparative Computational Experiments Results

The computational experiments results of estimating the embedded data hiding (estimations of image-containers distortions) using different the analyzed methods are given in Tables 2-4 and Figures 6-7.

Table 2 shows the computational experiments results of the data embedding into the container-image K1.Binary data are formed using the image B1 pixels (32×16 pixels).

Table 2: Estimations of the image-container K1 and extracted data distortions

Method, parameters	Container distortions		Extracted data distortions	
	MSE	SSIM	MSE	SSIM
The developed method, t_γ				
0,1	7,199E-03	9,964E-01	4,474E-02	9,992E-01
0,2	*7,798E-03*	*9,958E-01*	0,000E+00	1,000E+00
0,3	8,422E-03	9,951E-01	0,000E+00	1,000E+00
Koch-Zhao method, P				
0,5	2,886E-02	9,803E-01	3,587E-01	5,147E-01
5	*3,136E-02*	*9,766E-01*	0,000E+00	1,000E+00
25	4,373E-02	9,372E-01	0,000E+00	1,000E+00
Spread spectrum method, B_s				
4	5,924E-02	8,795E-01	0,000E+00	1,000E+00
8	*4,638E-02*	*8,827E-01*	0,000E+00	1,000E+00

The data of Table 2 show that the developed method provides more hidden data embedding (the best MSE and SSIM values of the measures were obtained) as compared with the Koch-Zhao method and the spread spectrum method. In Table 2 the best container-image distortions corresponding to the extracted data distortion absence are highlighted in italics.

Table 3 shows the computational experiments results of the same data embedding into the container-image K2.

Table 3: Estimations of the image-container K2 and extracted data distortions

Method, parameters	Container distortions		Extracted data distortions	
	MSE	SSIM	MSE	SSIM
The developed method, t_γ				
0,1	1,045E-02	9,965E-01	3,875E-02	1,000E+00
0,15	*1,090E-02*	*9,962E-01*	0,000E+00	1,000E+00
0,2	1,136E-02	9,958E-01	0,000E+00	1,000E+00
Koch-Zhao method, P				
0,5	1,256E-01	9,454E-01	3,641E-01	5,733E-01
5	*1,240E-01*	*9,435E-01*	0,000E+00	1,000E+00
25	1,217E-01	9,237E-01	0,000E+00	1,000E+00
Spread spectrum method, B_s				
4	9,583E-02	*9,176E-01*	0,000E+00	1,000E+00
8	*7,021E-02*	8,854E-01	0,000E+00	1,000E+00

The results in Table 3 also demonstrate the advantages of the developed embedding method.

Table 4 shows the computational experiments results of the same data embedding into the container-image K3.

Table 4: Estimations of the image-container K2 and extracted data distortions

Method, parameters	Container distortions		Extracted data distortions	
	MSE	SSIM	MSE	SSIM
The developed method, t_γ				
0,05	1,389E-02	9,956E-01	1,119E-01	9,999E-01
0,1	*1,450E-02*	*9,952E-01*	0,000E+00	1,000E+00
0,15	1,513E-02	9,948E-01	0,000E+00	1,000E+00
Koch-Zhao method, P				
0,5	1,065E-01	9,412E-01	3,510E-01	5,856E-01
5	*1,074E-01*	*9,391E-01*	0,000E+00	1,000E+00
25	1,140E-01	9,243E-01	0,000E+00	1,000E+00
Spread spectrum method, B_s				
4	8,517E-02	*9,551E-01*	0,000E+00	1,000E+00
8	*6,565E-02*	9,298E-01	0,000E+00	1,000E+00

The analysis of the results given in Table 4 also allows to makeconclusion that the developed embedding methodhas the advantages similar to the conclusions based on the analysis of the results displayed in the above tables.
Based on the results given in Tables 2-4, the graphs (Fig. 6) of the distortion estimations MSE and SSIM of the container-images K1, K2 and K3 are plotted.These graphsare plotted using the smallestcontainer-imagesdistortion while the extracted data have no distortions (the used values are shown in italicsin the tables).

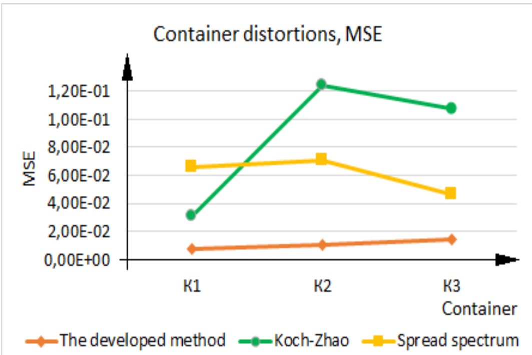

a

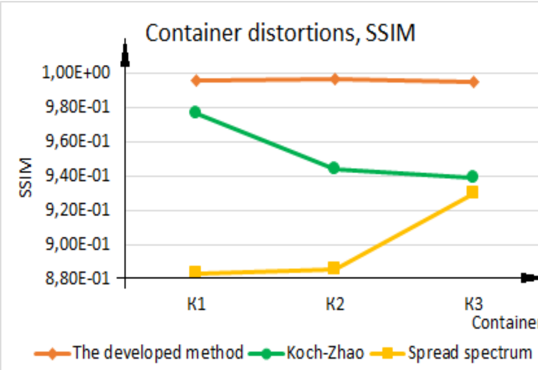

b

Figure 6: Graphics of containers-images K1, K2 and K3 distortions (containing the embedding data): a) MSE; b) SSIM

5. Conclusion

The results given in Tables 2-4 as well as the graphics shown in Figure 1 demonstrate that when applying the Koch-Zhao method and the spread spectrum method the distortions of container-images differ significantly while embedding in different container-images (we should remember that different container-images have different energy distributions over frequency intervals and over subsets of their projections onto subinterval matrices eigenvectors). Distortions after applying the Koch-Zhao method and the spread spectrum method are more significant than container-images distortions after using the developed method. Also different container-images distortions after applying the developed method differ slightly, it illustrates the adequacy of the developed decision rule which allow to take into account the various subinterval properties of container-images.

As an example of a container-images containing the embedded data the results of the hidden embedding of 4096 bits (image B1) into the container-image K1 are presented in Figure 7.

a

MSE=7,798E-03; SSIM=9,958E-01

MSE=3,136E-02; SSIM=9,766E-01 b

MSE=4,638E-02; SSIM=8,827E-01 c

Figure 7: Results of 4096 bits hidden embedding into the container image K1: a) the developed method, b) the Koch-Zhao method, c) the spread spectrummethod

The images shown in Figure 7 show that the distortions of container-image containing the embedded data is undistinguished for all analyzed methods. In these computational experiments the data were extracted without distortion.

The computational experiments results (Tables 2-4, Figures 3-7) illustrate that the developed hidden data embedding method has advantages in data embedding hiding as compared to Koch-Zhao method and spread spectrum method as when applying the developed method the container-images containing the embedded datahave smaller MSE distortion estimation and greater SSIM distortion estimation.Also the developed method application allows to extract the hidden embedded data without distortions.

6. Summary

Thereby we developed the method of the hidden data embedding into non-informative subsets of image projections onto subinterval matrices eigenvectors basing on a relative changes of given pair projections values in this article. This method allows to execute the hidden data embedding into images that causes the minor distortions of the container-image and the extracted data.

The performed computational experiments show that the developed method has advantages over the known Koch-Zhao method and the spread spectrum method. Computational experiments also show that the developed method allows to extract the embedded data without distortions while the data embedding causes the minor distortions of the container-images.

Acknowledgements

The work was carried out under the financial support of the Ministry of Education and Science in the frame-work of the state task of NRU BelSU (Project #8.2201.2017/4.6).

References

[1] Zhao J., Koch E. Embedding Robust Labels into Images for Copyright Protection. Processing of the Int. Congress on Intellectual Property Rights for Specialized Information, Knowledge and New Techniques, Munich-Vienna, Verlag, Aug. 1995, Pp. 242-251.

[2] Fridrich J. Combining Low-Frequency and Spread Spectrum Watermarking. Proc. Of the SPIE Conference of Mathematics of Data/Image Coding. Compression and Encription. 1998. Vol. 3456. P. 2-12.

[3] Raydhitya Yoseph, PSNR Comparison When Using LSB Steganography on Each RGB Color Component, IF 3058 Cryptography – Sem. II Year 2012/2013

[4] Khan Farhan Rafat and Muhammad Sher, On the Limits of Perfect Security for Steganography System. International Journal of Computer Science Issues (IJCSI). Volume 10, Issue 4, No. 2, July 2013, Pp. 121-126.

[5] Chincholkar A.A. and Urkude D.A. Design and Implementation of Image Steganography. Journal of Signal and Image Processing, Volume 3, Issue 3, pp. 111-113, 2012.

[6] Bin Li, Junhui He, Jiwu Huang, Yun Qing Shi. A Survey on Image Steganography and Steganalysis. Journal of Information Hiding and Multimedia Signal Processing, Vol. 2, Pp. 142-172, April 2011.

[7] Mandal J.K., Khamrui A. A Data-Hiding Scheme for Digital Image Using Pixel Value Differencing (DHPVD). Electronic System Design (ISED), International Symposium, Pp. 347-351, 2011.

[8] Konakhovich G.F., Puzyrenko A. Yu. Computer Steganography. Theory and practice. K., MK-Press, 288 p., 2006.

[9] Smith J., Comoskey B. Modulation and Information Hiding in Image. Information Hiding: First Int. Workshop “InfoHiding’96”, Springer as Lecture Notes in Computing Science, vol. 1174, 1996. Pp. 207-227.

[10] Chernomorets A.A., Zhilyakov E.G., Bolgova E.V., Petina M.A. and Kovalenko A.N. On Subband Embedding Resistance to Data Compression. Research Journal of Applied Sciences, 10: 403-406, 2015. DOI: 10.3923/rjasci.2015.403.406.

[11] Zhilyakov E.G., Konstantinov I.S., Chernomorets A.A., Bolgova E.V. Image Compression Method Using Subband Eigenvectors Decomposition. International Journal of Imaging and Robotics, 16(4): 69-81, 2016. URL: http://www.ceser.in/ceserp/index.php/iji/article/view/4639

[12] Zhilyakov E.G., Chernomorets A.A. Subband method of information secretive embedding into images. Belgorod State University Scientific Bulletin.History Political science Economics Information technologies. 13(132), pp. 216-221. 2012.

[13] Zhilyakov E.G., Chernomorets A.A., Bolgova E.V., Goloshchapova V.A. About subband embedding in colored images. Belgorod State University Scientific Bulletin. History Political science Economics Information technologies.1(198), pp. 158-162. 2015.

[14] Zhilyakov E.G., Chernomorets A.A., Bolgova E.V., Gahova N.N. About information subband embedding into space frequencies subareas of image-container. Journal Neurocomputers. 9, pp. 85-87. 2014.

[15] Bolgova E.V. The properties of subinterval matrices for a two-dimensional cosine transform. Information Systems and Technologies. 6(104), pp. 19-28, 2017.

[16] Bolgova E.V. About the eigenvalues of cosine transform subinterval matrices. Belgorod State University Scientific Bulletin. Economics Information technologies. 2(251), pp. 92-101. 2017.

[17] Bolgova E.V. About cosine transform energy concentration. Belgorod State University Scientific Bulletin. Economics Information technologies. 9(258), pp. 111-121. 2017

[18] Ahmed N., Rao K.R. Orthogonal Transforms for Digital Signal Processing. Springer-Verlag New York, Inc. Secaucus, NJ, USA, 1975.

[19] Wang Z., Bovik A.C., Sheikh H.R., Simoncelli E.P. Image quality assessment: From error visibility to structural similarity. IEEE Transactions on Image Processing, vol. 13, no. 4, pp. 600-612, Apr. 2004.